

# Assessment of Traffic-Related Air Pollution in Kirkuk City, Iraq Using Python-Based AERMOD and GIS

**Mohammed Hashim Ameen**

School of Civil Engineering, Engineering Campus, Universiti Sains Malaysia, Nibong Tebal, Seberang Perai Selatan, Pulau Pinang, Malaysia | Department of Environmental Engineering, Engineering College, Tikrit University, Tikrit, Iraq  
mohammed.hashim@tu.edu.iq

**Mastura Azmi**

School of Civil Engineering, Engineering Campus, Universiti Sains Malaysia, Nibong Tebal, Seberang Perai Selatan, Pulau Pinang, Malaysia  
cemastura@usm.my (corresponding author)

Received: 28 November 2025 | Revised: 20 December 2025 and 31 December 2025 | Accepted: 3 January 2026

Licensed under a CC-BY 4.0 license | Copyright (c) by the authors | DOI: <https://doi.org/10.48084/etasr.16563>

## ABSTRACT

Urban air pollution poses significant health and environmental concerns in rapidly developing cities such as Kirkuk, Iraq. This study examines the spatial distribution and intensity of PM<sub>2.5</sub>, NO<sub>x</sub>, and CO along the Kirkuk-Baghdad Road using AERMOD integrated with Python-based GIS tools. Emission rates were calculated from vehicle counts, speeds, and emission factors during the peak traffic hours of 8-10 AM and 5-7 PM. The model incorporated meteorological data, terrain characteristics, and emission sources to simulate pollutant dispersion patterns. The results revealed that pollutant concentrations near traffic hotspots frequently exceeded the proposed limits. Peak concentrations reached 125 µg/m<sup>3</sup> for PM<sub>2.5</sub> at K-B R16, 21 ppm for CO, and 1.00 ppm for NO<sub>x</sub> at K-B R18. Heavy-duty vehicles, especially trucks and motorcycles, contributed significantly to elevated concentrations. Weather conditions and topography influenced dispersion patterns substantially. Python-based spatial analysis facilitated efficient processing of traffic and monitoring data, enabling visualization of pollution hotspots and comprehensive mapping across the study area. This research demonstrates the value of integrated GIS-AERMOD approaches for urban air quality assessment and provides insights for traffic management and emission-reduction strategies to protect public health.

*Keywords-traffic emissions; air pollution; GIS; AERMOD; dispersion modeling; python*

## I. INTRODUCTION

Urban air pollution has become one of the most significant issues in the rapidly growing cities [1]. Several cities, including Kirkuk in Iraq, are experiencing high rates of traffic congestion due to the increase in economic activities and population density, which directly emits harmful pollutants [2, 3]. Among such pollutants, a particular concern is fine particulate matter (PM<sub>2.5</sub>), nitrogen oxides (NO<sub>x</sub>), and carbon monoxide (CO) that can reach deep into the respiratory system and cause cardiovascular and lung diseases and have an overall negative impact on the environment [4-6]. Large road networks, particularly the Kirkuk-Baghdad Road, act as important transport networks and are also a consistent place of pollutant emissions based on the number of vehicles, the type of fleet, and traffic patterns [7]. Since standard air-quality surveillance is not sufficient to describe the multidimensional nature of quantity and time dispersion of emissions [8], complex

modeling methods have been adopted to assess the distribution of pollutants and determine where the possible exposure hotspots are [9]. AERMOD is a well-known atmospheric dispersion model, which offers an effective framework for simulating the distribution of pollutants under different meteorological and terrain conditions [10-12]. By combining this model with Python-based GIS tools, the analytical ability can be improved, as these tools allow automated processing of data [13, 14]. AERMOD applications in rapidly urbanizing cities, such as Kirkuk, Iraq, remain limited, especially when integrated with Python and GIS for traffic-related air pollution mapping and analysis. This combined strategy can help investigate the role of peak-hour vehicle fleets in increasing pollutant levels [15], especially the impact of trucks and motorcycles [16]. It can also be used to understand the effect of local weather conditions on dispersion processes [17].

In this regard, the proposed study employs a combined AERMOD-Python-GIS methodology to provide a detailed numerical and spatial analysis of the impact of traffic pollution on air quality along the Kirkuk-Baghdad Road during the morning and evening rush hours. The objectives of the study are:

- To calculate spatiotemporal changes in the concentrations of PM<sub>2.5</sub>, NO<sub>x</sub>, and CO using AERMOD.
- To identify the hotspots and factors that affect the pollution hotspots/them.
- To compare the estimated concentrations with the WHO air quality standards.
- To provide evidence-based recommendations for town planning and traffic control.

The present study addresses the identified research gap by demonstrating that combined Python-AERMOD-GIS can be an effective tool in forming emission-reduction policy and preserving the health of the population in rapidly urbanizing environments.

II. METHOD

A. Study Area

The study area, Kirkuk City, is situated in Iraq's Kirkuk province, roughly 250 km north of Baghdad [18]. The coordinates of the study area are E: 445,744.63, N: 3,535,902.33, as shown in Figure 1. Due to its advantageous location, Kirkuk experiences significant traffic from both private and commercial vehicles. Urban noise levels and air quality are significantly impacted by this high traffic intensity [19, 20].

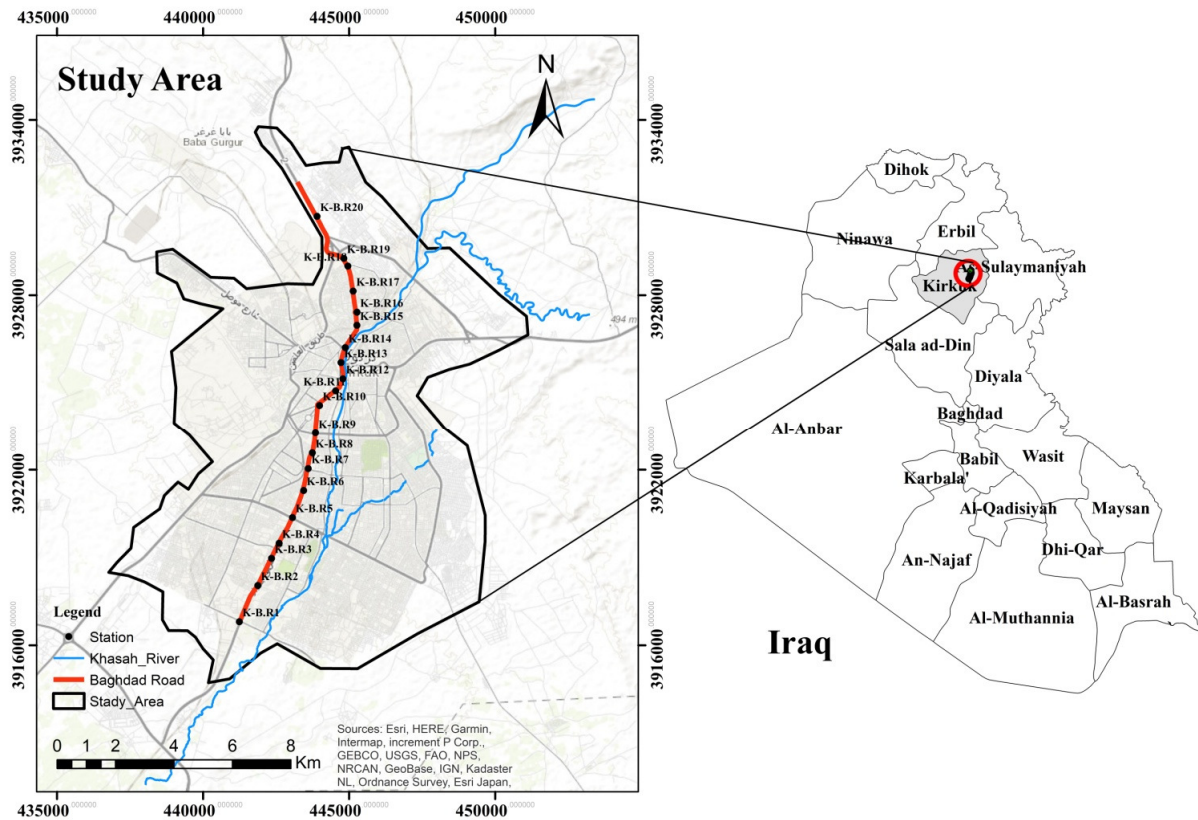


Fig. 1. Location map of Kirkuk City, Iraq, showing the study area.

B. Input Data Collection

The main input data, including the average speeds, number of vehicles, and the emission factors, were collected to estimate traffic emissions. Based on the findings in [20], the emission rate of each pollutant was calculated using (1). Emission rate is defined as the product of the emission factor, the average vehicle speed ( $V_m$ ), and the number of vehicles ( $N$ ) passing through a road section per day:

$$Emission\ rate\ \left(\frac{g}{s}\right) = \frac{EF\left(\frac{g}{km}\right) \cdot V_m\left(\frac{km}{h}\right) \cdot N}{3600\left(\frac{s}{h}\right)} \quad (1)$$

The emission factors were selected based on vehicle type (passenger cars, trucks, and motorcycles). The average speed range (20-60 km/h) was measured in the field. Based on the local fuel quality (0.5-1 Euro -equivalent diesel and gasoline), the following specific emission factors were used (g/km/vehicle): For PM<sub>2.5</sub>, emission factors were 0.025 for

cars, 0.180 for trucks, and 0.042 for motorcycles. For NO<sub>x</sub>, the corresponding values were 0.650 for cars, 5.20 for trucks, and 0.135 for motorcycles. For CO, emission factors were 1.20 for cars, 2.80 for trucks, and 5.60 for motorcycles.

### C. Meteorological Data Processing

The processing of meteorological data was performed in accordance with EPA guidelines using AERMET. Hourly surface and upper-air data quality-checked at the Kirkuk station were combined and used to determine the required parameters. The meteorological data of the year 2023 that had undergone preprocessing were directly entered into AERMOD to consider changes in seasons and times of the day. Table I presents the wind velocity category data used to determine the local atmospheric stability frequency distribution. The stability class ranges from Extremely unstable to Stable.

TABLE I. WIND VELOCITY CATEGORIES AND ATMOSPHERIC STABILITY

Wind velocity (m/s)	Class
1.54	A—Extremely unstable
3.09	B—Moderately unstable
5.14	C—Rarely unstable
8.23	D—Neutral
10.23	E—Stable

### D. Variables and Contributing Factors

Vehicle numbers, types, consumption of fuel, and emission factors for important pollutants, such as PM<sub>2.5</sub>, NO<sub>x</sub>, and CO, were used to estimate traffic emissions.

### E. Data Preprocessing

The number of vehicles in the traffic was classified by type and time of day. The data on the meteorological conditions in the local weather stations were formatted to the input requirements of AERMOD and were standardized to all receptor points to ensure uniformity. The Variance Inflation Factor (VIF) test, with a cut-off of 10, was applied to enhance efficiency and reduce redundancy. Multicollinearity is determined by VIF in regression analysis to estimate the level of increase in the variance of a regression coefficient because of the correlation with other variables. High correlation coefficients (VIF > 10) were deleted, which led to an overall model enhancement and a reduction in the number of variables in the dataset:

$$VIF = \frac{1}{1-R_i^2} \quad (2)$$

where  $R_i^2$  is the correlation coefficient of the  $i^{th}$  independent variable.

### F. Dispersion Model Development

#### 1) Gaussian Dispersion Model

AERMOD estimates the concentration of pollutants using the Gaussian plume equations, as defined in (3). The

integration of this model helped analyze the impacts of the emitted traffic on the extent of air pollution in Kirkuk City.

$$C_p = \frac{Q}{2\pi Du} \exp\left(-\frac{d^2}{2\sigma_y^2}\right) \left( \exp\left(-\frac{(z-H)^2}{2\sigma_z^2}\right) + \exp\left(-\frac{(z+H)^2}{2\sigma_z^2}\right) \right) = \frac{Q}{2\pi Du} \exp\left(-\frac{d^2}{2\sigma_y^2}\right) \cosh\left(\frac{zH}{\sigma_z}\right) \quad (3)$$

#### 2) Dispersion Modeling of Traffic Emissions with AERMOD

AERMOD is used to develop a model to estimate emissions of PM<sub>2.5</sub>, NO<sub>x</sub>, and CO from vehicles on Baghdad Road. The key equation in the model is:

$$C(x) = \frac{Q}{2\pi\sigma_y\sigma_z} \exp\left(-\frac{y^2}{2\sigma_y^2}\right) \exp\left(-\frac{z^2}{2\sigma_z^2}\right) \quad (4)$$

where  $C(x)$  is the concentration at the receptor,  $Q$  is the emission rate, and  $\sigma_y$ ,  $\sigma_z$  are the horizontal and vertical dispersion coefficients, respectively. These coefficients depend on atmospheric stability and distance from the source, expressed as:

$$\sigma_y = a_y x^{b_y} \sigma_z = a_z x^{b_z} \quad (5)$$

For building downwash, adjustments to the dispersion coefficients are applied as:

$$\sigma_y = \sigma_{y0} + \Delta\sigma_y \sigma_z = \sigma_{z0} \frac{H+\Delta h}{H} \quad (6)$$

where  $H$  is the building height and  $\Delta h$  is the plume's vertical position Standard Deviation (SD). Downwash correction is applied as:

$$\Delta\sigma_y = k_y S w, \Delta h = k_z H \quad (7)$$

In complex terrain, vertical dispersion is adjusted for plume lifting, described by:

$$\sigma_z = \sigma_{z0} \left(1 + \frac{\Delta h}{h_c - h_t}\right) \quad (8)$$

where  $h_c$  is the plume centerline height and  $h_t$  is the terrain height.

#### 3) Road Source Representation in AERMOD

The Kirkuk–Baghdad Road was modeled in Python using AERMOD with the VOLUME source type, divided into 20 segments (500–750 m) with  $\sigma_{y0} = 50$  m,  $\sigma_{z0} = 3$  m, and a 0.5 m release height to represent vehicle emissions. This setup follows EPA guidelines for receptors 10–50 m from the road.

### G. Model Validation

Observations of 20 temporary monitoring stations and EPA-recommended statistical metrics were used to evaluate model performance. The findings demonstrate that modeled and measured concentrations are strongly related, the  $R^2$  varies between 0.693 and 0.999, RMSE ranges from 0.14 to 11.27, normalized MSE ranges from 0.063 to 0.885, and the agreement index is 0.968 for PM<sub>2.5</sub>, NO<sub>x</sub>, VOC, and CO, indicating the strength and reliability of the model.

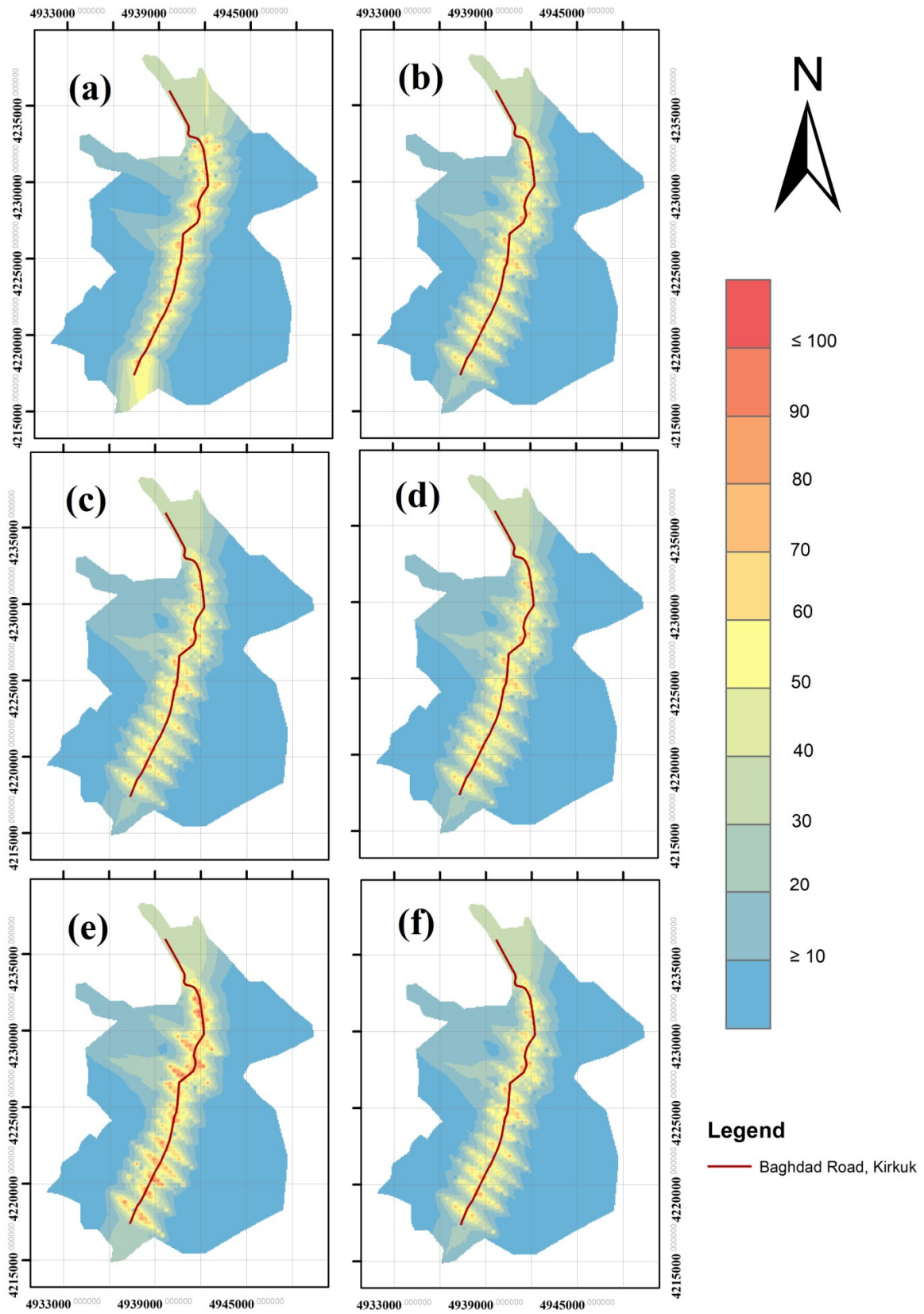


Fig. 2. Average PM<sub>2.5</sub> spatial distribution: (a) evening, (b) morning, (c) Saturday, (d) Thursday, (e) Tuesday, and (f) Friday.

III. RESULTS AND DISCUSSION

A. AERMOD-Based Distribution of PM<sub>2.5</sub>

The highest recorded concentration was observed at station K-B. R16, with peak, mean, and SD values of 125.00 µg/m<sup>3</sup>, 96.39 µg/m<sup>3</sup>, and 13.75 µg/m<sup>3</sup>, respectively, indicating intense localized pollution levels. In contrast, the lowest concentration was recorded at station K-B. R5, with minimum, mean, and SD values of 66.00 µg/m<sup>3</sup>, 85.13 µg/m<sup>3</sup>, and 13.13 µg/m<sup>3</sup>, respectively. At 12 of 20 receptor points (60%) PM<sub>2.5</sub> exceeded the WHO limit (15 µg/m<sup>3</sup>) by 4.4–8.3 times, with a peak value of 125 µg/m<sup>3</sup>.

This variability suggests high spatial variation in PM<sub>2.5</sub> concentration. Some stations, including K-B. R8 and K-B. R19 had extended histograms, indicative of a varying signal strength of PM<sub>2.5</sub>, due temporary change in the physical environment or the human activities. For instance, K-B. R10 and K-B. R2 had relatively lower and more constant PM<sub>2.5</sub>

levels, which indicates constant pollution sources or environmental disturbance. These differences are illustrated in Figure 2.

1) Temporal Analysis for PM<sub>2.5</sub>

When daily PM<sub>2.5</sub> concentration was compared, both mean and dispersion values varied significantly, as presented in Table II and Figure 3. Saturday had the highest mean PM<sub>2.5</sub> concentration of 95.06 µg/m<sup>3</sup>, with a relatively low SD of 2.65, indicating consistently elevated pollutant levels. In contrast, Friday had the lowest mean concentration of 76.30 µg/m<sup>3</sup>, but with a relatively higher SD of 4.80 µg/m<sup>3</sup> compared to the concentration of the pollutants. Saturday and Thursday exhibited lower PM<sub>2.5</sub>, while Tuesday and Friday had higher PM<sub>2.5</sub>. The observed high emission values on Saturday and Thursday relate to stable emission sources or atmospheric conditions, while sharp variations on Tuesday and Friday can be explained by variable or temporary factors.

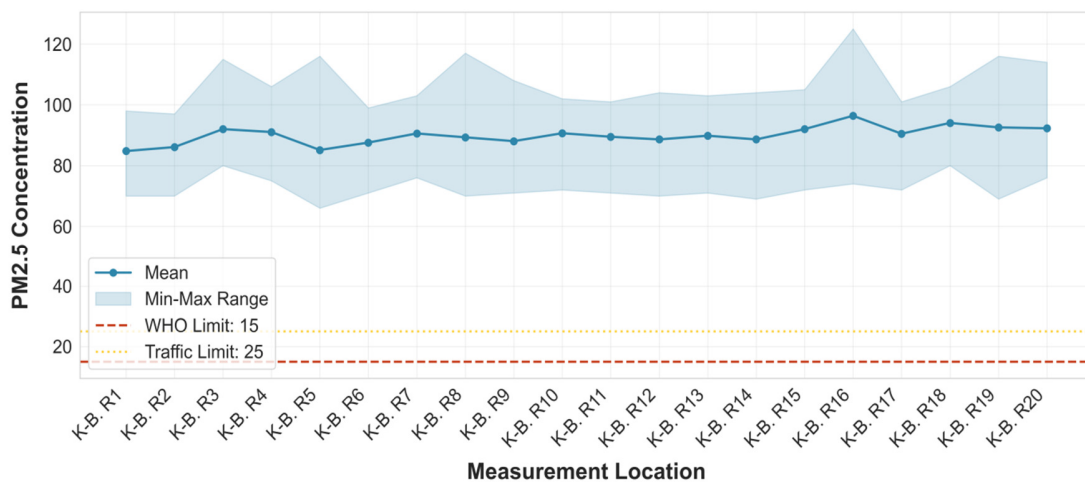


Fig. 3. PM<sub>2.5</sub> pollution survey statistics and measured data along the Baghdad Road of Kirkuk City.

TABLE II. PM<sub>2.5</sub> CONCENTRATIONS ALONG BAGHDAD ROAD IN KIRKUK CITY

Day	Mean	SD	Min. value (µg/m <sup>3</sup> )	Max. value (µg/m <sup>3</sup> )
Friday	76.30	4.80	69.50	90.00
Saturday	95.06	2.65	90.33	99.00
Thursday	87.66	2.63	81.86	93.57
Tuesday	91.60	4.30	83.25	101.25

2) Temporal Analysis by Time of Day

The obtained PM<sub>2.5</sub> data during day time demonstrated significant variations in concentration. The analysis of PM<sub>2.5</sub> concentrations during daytime showed a distinct pattern; in the morning, the mean PM<sub>2.5</sub> level was 91.67 µg/m<sup>3</sup>, with an SD value of 3.67 µg/m<sup>3</sup> and with minimum and maximum values of PM<sub>2.5</sub> concentrations ranging from 85.73 µg/m<sup>3</sup> to 102.73 µg/m<sup>3</sup>, respectively. This suggests slightly higher pollution levels with moderate variability. In the evening, the mean concentration decreased to 88.42 µg/m<sup>3</sup>, with an SD of 3.14 µg/m<sup>3</sup> and with minimum and maximum values ranging from

81.25 µg/m<sup>3</sup> to 94.08 µg/m<sup>3</sup>. The results indicate that the PM<sub>2.5</sub> concentration was higher in most parts of the day, however, with moderate changes during the morning hours. The reduction in PM<sub>2.5</sub> concentrations at night indicates a reduction in traffic, weather conditions, or any other condition within the area at different periods of the day. The temporal analysis summary is presented in Table III.

TABLE III. RESULTS OF PM<sub>2.5</sub> TEMPORAL ANALYSIS ALONG THE BAGHDAD ROAD IN KIRKUK CITY

Time	Mean	SD	Min. value (µg/m <sup>3</sup> )	Max. value (µg/m <sup>3</sup> )
Morning	91.67	3.67	85.73	102.73
Evening	88.42	3.14	81.25	94.08

3) Comparison with Air Quality Standards

Table IV presents the spatial distribution of PM<sub>2.5</sub> concentrations compared to established safety limits based on location categories [20, 21]. The comparative analysis helps identify areas that exceeded the proposed limits and require immediate action.

TABLE IV. COMPARATIVE ANALYSIS FOR PM<sub>2.5</sub> LEVELS BASED ON LOCATION CATEGORIES [20, 21]

Location category	Max. PM <sub>2.5</sub> (annual mean, µg/m <sup>3</sup> )	Max. PM <sub>2.5</sub> (24-h mean, µg/m <sup>3</sup> )
Urban	≤ 5	≤ 15
Rural	≤ 5	≤ 15
Industrial	Varies by Industry (typically ≤ 5)	Varies by industry (typically ≤ 15)
Sensitive (schools, hospitals)	≤ 5	≤ 10
Natural (parks, wilderness)	Aims for low levels (typically ≤ 5)	Aligned with urban standards (≤ 15)

### B. Spatial Distribution of CO Concentrations

The spatial distribution of the mean CO concentrations was also assessed across different measurement locations, as depicted in Figure 4. The results revealed a significant difference in concentration levels with respect to site conditions. Station K-B. R18 had the highest CO concentration with an average CO of 8.26 ppm, an SD of 4.87 ppm, and a maximum CO concentration of 21.00 ppm. This indicates a significant local pollution concentration. In contrast, the lowest levels were recorded at station K-B. R1, with mean, SD, and minimum CO concentrations of 2.04 ppm, 0.77 ppm, and 1.00 ppm, respectively.

These variations indicate a presence of relatively high spatial differentiation in the CO concentration in the study area. The difference in CO at stations K-B. R18 and K-B. R17 can be attributed to the variability of the intensity of the pollutants, which depends upon variability in environmental factors such as the traffic volume and type. In contrast, the CO levels at stations K-B. R1 and K-B. R2 were relatively constant, suggesting similar environmental conditions or low traffic during the time of measurement. The results also demonstrate the effectiveness of a site-specific approach to pollution dynamics and for developing targeted mitigation strategies, as shown in Figure 5.

#### 1) Daily Variations in CO Concentrations

The daily CO concentration trends along the Baghdad Road in Kirkuk City, depicted in Table V, show significant variations. The average CO level was the highest on Tuesday, with mean and SD CO concentration values of 7.13 ppm and 1.98 ppm, respectively. The most stable conditions were observed on Thursday, with a minimum SD of 1.68 ppm and a mean of CO concentrations of 6.38 ppm. These findings suggest that traffic congestion and speed affect CO concentrations, with Tuesday facing the highest pollution and Thursday the most stable concentration.

#### 2) Time-of-Day Variations in CO Concentrations

As presented in Table VI, the morning hours recorded a mean CO level of 6.77 ppm and an SD of 1.86 ppm, with minimum and maximum CO concentrations ranging from 2.45 ppm to 9.82 ppm, respectively. In the evening, the CO concentration was slightly higher with a mean value of 6.78 ppm, an SD of 2.09 ppm, and minimum and maximum CO concentrations ranging from 1.67 ppm to 9.58 ppm, respectively. There were minor fluctuations in the CO concentrations throughout the day, with similar CO

concentrations recorded during morning and evening hours. However, the SD during the evening hours was slightly higher due to the increase in traffic flow during the period.

TABLE V. CO CONCENTRATIONS DURING DAYTIME ON BAGHDAD ROAD IN KIRKUK CITY

Day	Mean	SD	Min. value (ppm)	Max. value (ppm)
Friday	6.20	1.93	1.50	9.00
Saturday	6.94	2.20	2.00	9.50
Thursday	6.38	1.68	1.86	8.29
Tuesday	7.13	1.98	2.38	9.75

TABLE VI. CO CONCENTRATIONS BY TIME ON BAGHDAD ROAD IN KIRKUK CITY

Time	Mean	SD	Min. value (ppm)	Max. value (ppm)
Morning	6.77	1.86	2.45	9.82
Evening	6.78	2.09	1.67	9.58

### C. Spatial Distribution of NO<sub>x</sub>

Station K-B. R11 recorded the highest NO<sub>x</sub> concentrations with a maximum value of 0.45 ppm and an SD of 0.24. Station including K-B. R9 also recorded high levels of NO<sub>x</sub> concentrations, with mean NO<sub>x</sub> concentrations of 0.41 ppm, and minimum and maximum NO<sub>x</sub> concentrations ranging from 0.05 to 0.90 ppm, respectively. Similarly, station K-B. R17 had a mean NO<sub>x</sub> concentration of 0.43 ppm, with minimum and maximum NO<sub>x</sub> concentrations ranging from 0.10 to 1.00 ppm. This spatial distribution indicates the local pollution hot spots, due to traffic congestion and the presence of urban structure. Figure 6 visualizes these variations across the study area. Figure 7 shows processed data of the NO<sub>x</sub> concentrations along the Baghdad Road of Kirkuk. The observed temporal patterns are consistent with traffic-dominated urban areas, with evening peaks driven by rush-hour congestion and reduced atmospheric mixing. NO<sub>x</sub> concentrations were converted to NO<sub>2</sub> using a typical urban NO<sub>x</sub>/NO<sub>2</sub> ratio of 1.5, yielding a peak NO<sub>2</sub> level of 0.67 ppm, which substantially exceeds the WHO 24-h guideline of 0.013 ppm. In contrast, sites including K-B. R4 recorded lower mean concentrations of 0.26 ppm, SD of 0.23, ranging from 0.00 to 0.60 ppm, indicating more stable and moderate pollutant levels. Similarly, K-B. R10 exhibited a mean NO<sub>x</sub> concentration of 0.26 ppm, with a limited variability ranging from 0.00 to 0.50 ppm. These findings highlight the role of emission dynamics and localized traffic conditions in shaping NO<sub>x</sub> spatial distribution patterns.

#### 1) NO<sub>x</sub> Temporal Analysis by Day

On Friday, NO<sub>x</sub> levels averaged 0.24 ppm (SD = 0.14 ppm, range: 0.00–0.40 ppm), reflecting relatively low and stable variability. Saturday showed a slight increase in the mean concentration to 0.30 ppm (SD = 0.07 ppm, range: 0.15–0.45 ppm), followed by Thursday with a mean concentration of 0.35 ppm (SD = 0.08 ppm, range: 0.24–0.50 ppm). Tuesday exhibited the highest mean concentration of 0.42 ppm (SD = 0.07 ppm, range: 0.28–0.51 ppm), suggesting higher levels of pollution and lower variability. Table VII presents the NO<sub>x</sub> concentration by day.

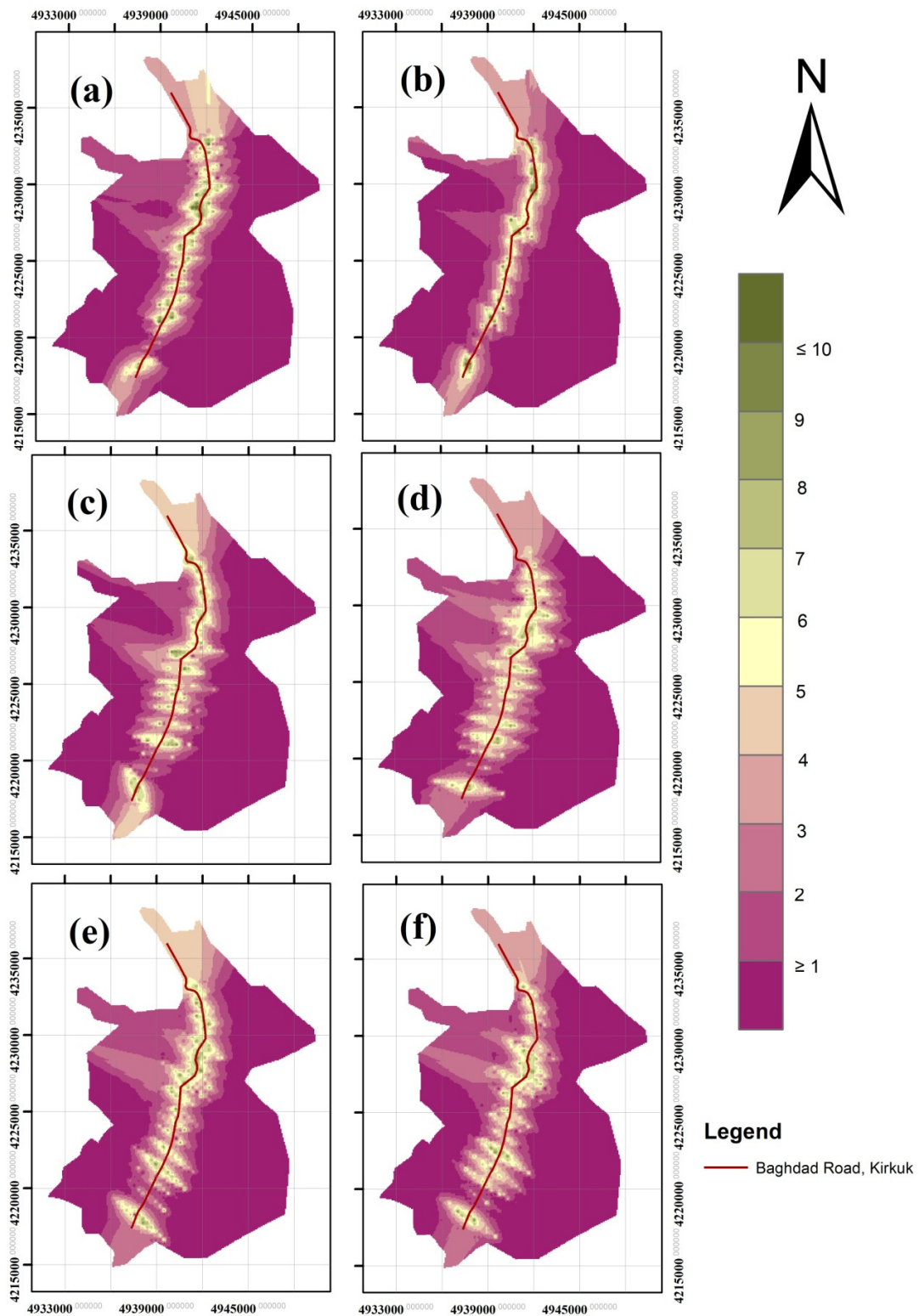


Fig. 4. Average CO spatial distribution: (a) evening, (b) morning, (c) Saturday, (d) Thursday, (e) Tuesday, and (f) Friday.

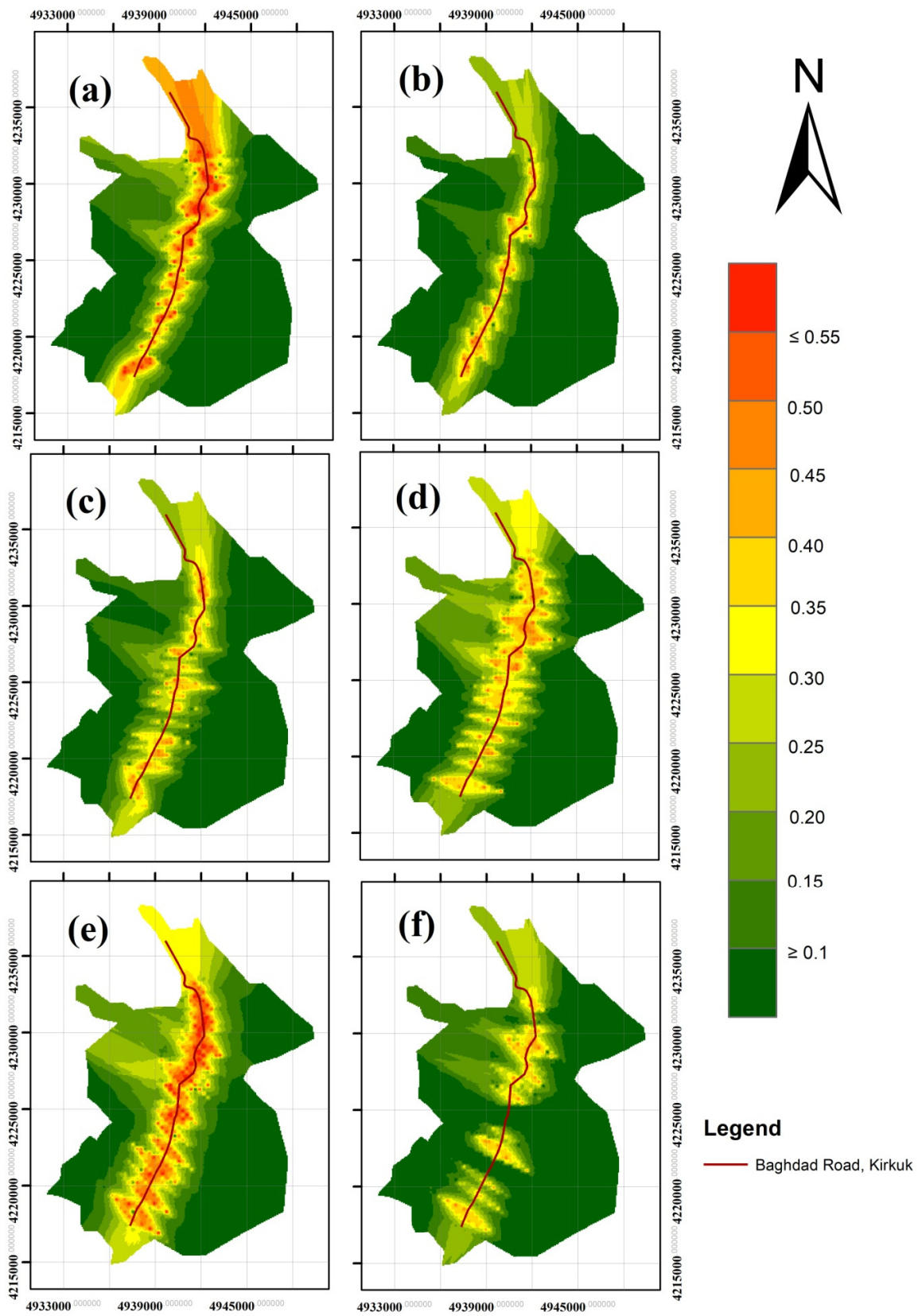


Fig. 5. Average NO<sub>x</sub> spatial distribution: (a) evening, (b) morning, (c) Saturday, (d) Thursday, (e) Tuesday, and (f) Friday.

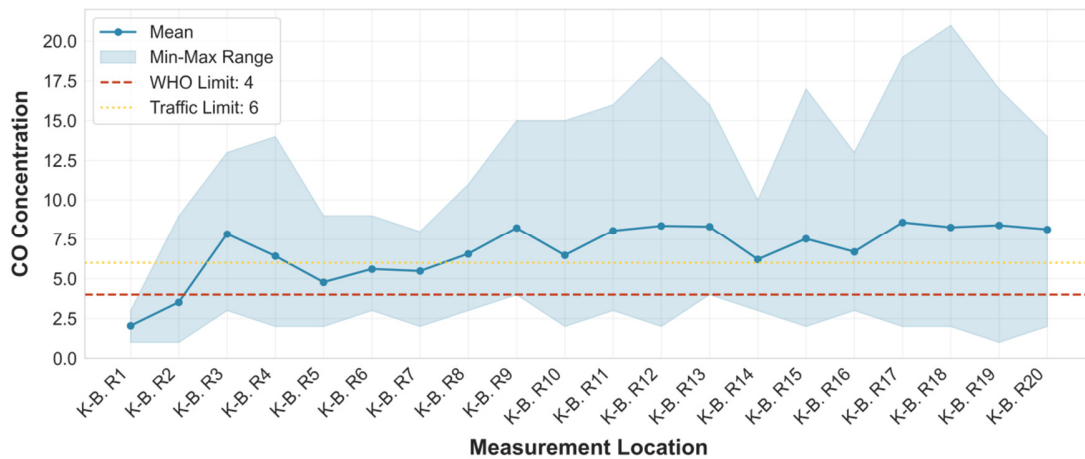


Fig. 6. CO pollution survey statistics and measured data along the Baghdad Road in Kirkuk City.

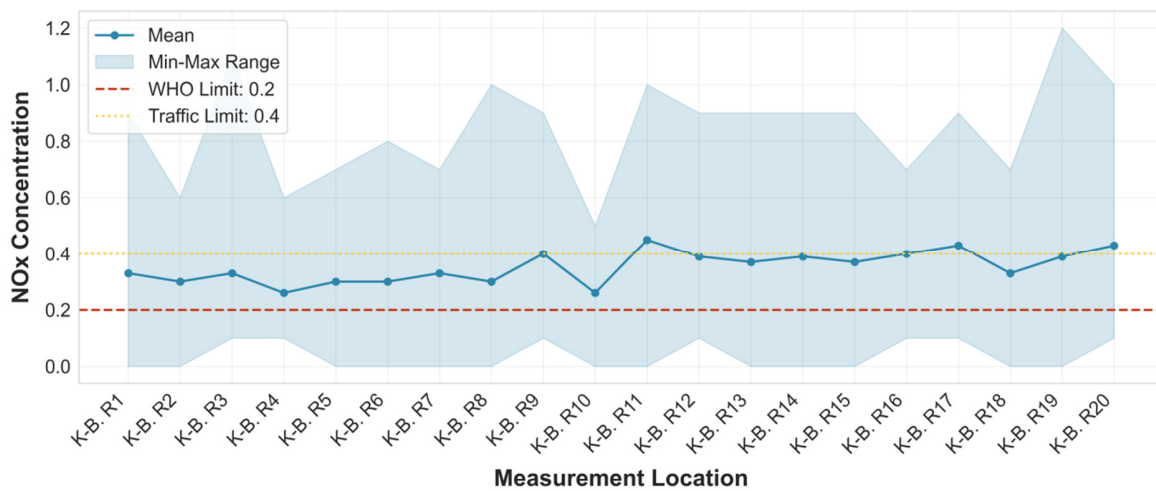


Fig. 7. NO<sub>x</sub> pollution survey statistics and measured data along the Baghdad Road in Kirkuk City.

2) Temporal Analysis by Time of Day

In the morning, the mean concentration was 0.29 ppm (SD = 0.07, range: 0.17–0.41 ppm), indicating relatively stable and lower pollution levels. In contrast, the evening period showed a higher mean concentration of 0.41 ppm (SD = 0.11, range: 0.21–0.58 ppm), with increased variability. The statistics of the NO<sub>x</sub> concentrations according to the time of day are presented in Table VIII.

AERMOD-based studies have concluded that dispersion models are able to spatially resolve the traffic-induced hotspots, although with varying degrees of accuracy depending on configuration and validation information [22]. Similar analyses [23] also demonstrate the presence of the highest pollutants concentrated around heavy traffic movement, confirming the findings of the present study. Various studies on near-road conditions suggest the nonlinear relationship between emissions and concentrations, supporting the designation of heavy vehicles as major contributors to elevated concentrations along the Kirkuk–Baghdad Road [6].

TABLE VII. NO<sub>x</sub> CONCENTRATION BY DAY ALONG THE BAGHDAD ROAD IN KIRKUK CITY

Day	Mean	SD	Min. value (ppm)	Max. value (ppm)
Friday	0.24	0.14	0.00	0.40
Saturday	0.30	0.07	0.15	0.45
Thursday	0.35	0.08	0.24	0.50
Tuesday	0.42	0.07	0.28	0.51

TABLE VIII. NO<sub>x</sub> CONCENTRATION BY TIME ALONG THE BAGHDAD ROAD IN KIRKUK CITY

Time	Mean	SD	Min. value (ppm)	Max. value (ppm)
Morning	0.29	0.07	0.17	0.41
Evening	0.41	0.11	0.21	0.58

IV. CONCLUSIONS

The study presented a quantitative and detailed evaluation of the role of road traffic on air pollution along Baghdad Road in Kirkuk City, Iraq. A combination of the proposed

mathematical model, AERMOD dispersion simulations, Python programming, and GIS-based spatial analysis proved to be an effective and reliable solution for identifying pollutant dispersion patterns and pollution hotspots.

The findings indicate that vehicle emissions are the major sources of high levels of CO, NO<sub>x</sub>, and PM<sub>2.5</sub>, particularly along the high traffic density zones. Although the average pollutant concentrations at various stations were within the regulatory limits, local spikes around major roadways were consistent, suggesting higher exposure risks in a short time period. The findings also suggest that the meteorological conditions and urban topography in Kirkuk City are very important in the control of the traffic-induced pollutants. Also, the peak hours of traffic in the city represent the most vulnerable sectors, putting people at risk of exposure.

The results highlighted that there is an urgent need to implement pollution mitigation strategies, including the introduction of more stringent maintenance checks, the introduction of cleaner, higher-quality fuel, the optimization of traffic routes and traffic flow, the systematic incorporation of air-quality improvement measures into the city environment, and the design of the roads.

Moreover, this study confirms the effectiveness of Python-based AERMOD modeling with GIS visualization as an effective decision support tool in the management of air-quality in urban areas. The proposed framework can be applied to other cities that are rapidly urbanizing, facilitating evidence-based policy-making. Future research should broaden this methodology and evaluate the combined effects of transportation networks on the air quality in urban areas, as well as the establishment of long-term pollution reduction strategies and the promotion of sustainable urban development.

#### ACKNOWLEDGMENT

The authors express their sincere gratitude to Dr. Eapak for her valuable assistance and acknowledge the use of traffic data from the Kirkuk Traffic Department.

#### REFERENCE

- [1] S. Mahmood, A. Ali, and H. J. Jumaah, "Geo-Visualizing the Hotspots of Smog-Induced Health Effects in District Gujranwala, Pakistan: A Community Perspective," *Environmental Monitoring and Assessment*, vol. 196, no. 5, May 2024, Art. no. 457, <https://doi.org/10.1007/s10661-024-12619-w>.
- [2] M. H. Ameen, M. Azmi, and H. J. Jumaah, "Evaluating Exposure to Road Traffic Air and Noise Pollution: A Comprehensive Review of Assessment Methods," *Tikrit Journal of Engineering Sciences*, vol. 32, no. 2, pp. 1–19, May 2025, <https://doi.org/10.25130/tjes.32.2.9>.
- [3] H. J. Jumaah, M. H. Ameen, S. Mahmood, and S. J. Jumaah, "Study of Air Contamination in Iraq Using Remotely Sensed Data and GIS," *Geocarto International*, vol. 38, no. 1, Dec. 2023, Art. no. 2178518, <https://doi.org/10.1080/10106049.2023.2178518>.
- [4] I. Manisalidis, E. Stavropoulou, A. Stavropoulos, and E. Bezirtzoglou, "Environmental and Health Impacts of Air Pollution: A Review," *Frontiers in Public Health*, vol. 8, Feb. 2020, Art. no. 14, <https://doi.org/10.3389/fpubh.2020.00014>.
- [5] H. J. Jumaah, M. A. Dawood, T. A. Abd Alreza, and M. A. Meteab, "Air Pollution Landscape in Iraq: A Sentinel-5P Based Assessment of key Atmospheric Pollutants," *DYSONA - Applied Science*, vol. 7, no. 1, Jan. 2026, <https://doi.org/10.30493/das.2025.539377>.
- [6] M. H. Askariyeh, M. Venugopal, H. Khreis, A. Birt, and J. Zietsman, "Near-Road Traffic-Related Air Pollution: Resuspended PM<sub>2.5</sub> from Highways and Arterials," *International Journal of Environmental Research and Public Health*, vol. 17, no. 8, Apr. 2020, Art. no. 2851, <https://doi.org/10.3390/ijerph17082851>.
- [7] Y. H. Mahmood, R. T. Ahmed, and M. A. Najemalden, "Air Quality in Kirkuk Regarding PM<sub>10</sub> Concentrations," *Review of International Geographical Education Online*, vol. 11, no. 5, pp. 3912–3918, Jan. 2021.
- [8] R. S. Sokhi *et al.*, "Advances in Air Quality Research – Current and Emerging Challenges," *Atmospheric Chemistry and Physics*, vol. 22, no. 7, pp. 4615–4703, Apr. 2022, <https://doi.org/10.5194/acp-22-4615-2022>.
- [9] L. R. F. Henneman, I. C. Dedoussi, J. A. Casey, C. Choirat, S. R. H. Barrett, and C. M. Zigler, "Comparisons of Simple and Complex Methods for Quantifying Exposure to Individual Point Source Air Pollution Emissions," *Journal of Exposure Science & Environmental Epidemiology*, vol. 31, no. 4, pp. 654–663, Jul. 2021, <https://doi.org/10.1038/s41370-020-0219-1>.
- [10] V. H. Shukla, H. S. Syed, and V. R. Shah, "A Review on the Performance of AERMOD Software for Different Air Pollutant Sources under Indian Context," *International Journal of Darshan Institute on Engineering Research and Emerging Technologies*, vol. 10, no. 2, Jan. 2022, Art. no. 17, <https://doi.org/10.32692/IJDI-ERET/10.2.2021.2104>.
- [11] A. Adimi, A. Nohegar, Z. Sazvar, and M. Behrouzi, "Effect of Inversion on Pollutant Dispersion of the Steel Factory," *Air Quality, Atmosphere & Health*, vol. 18, no. 7, pp. 1905–1918, Jul. 2025, <https://doi.org/10.1007/s11869-025-01736-1>.
- [12] P. Cau, D. Muroi, G. Satta, C. Milesi, and C. Casari, "AERQ—A Web-Based Decision Support Tool for Air Quality Assessment," *Applied Sciences*, vol. 15, no. 4, Feb. 2025, Art. no. 2045, <https://doi.org/10.3390/app15042045>.
- [13] H. Jumaah, K. Valizadeh Kamran, A. Ghanbari, and M. Jeihouni, "Development of GIS-Based Box Model Tool for Air Quality Mapping with Python and ArcGIS Pro in Kirkuk City, Iraq," *International Journal of Engineering and Geosciences*, vol. 11, no. 1, pp. 212–225, Oct. 2025, <https://doi.org/10.26833/ijeg.1710723>.
- [14] S. A. A. Hashmi, "The Python Paradigm: A Twenty-Five Year Retrospective on its Strategic Dominance Over Contending Languages and its Ascendancy as the Indispensable Engine of Modern AI, IoT, GIS, and Cybersecurity," Oct. 2025, <https://doi.org/10.5281/ZENODO.17282464>.
- [15] G. S. Mohammad, "Signal Timing for LCV Trucks on a Road Network Using Reinforcement Learning," Master's thesis, York University, Toronto, Canada, 2025.
- [16] Y. Zhong, H. Wang, T. Jing, Y. Yang, H. Zou, and Y. Jin, "Unveiling the Spatiotemporal Evolution Characteristics of Urban Residents' Travel Patterns and Spillover Effects of Jobs-Housing Spaces in China Based on Multi-Source Data," SSRN, 2025, <https://doi.org/10.2139/ssrn.5179218>.
- [17] A. Bredder, "Modeling the Impact of Particulate Matter on Respiratory Hospital Admissions in Alaska During the Wildfire Season," PhD dissertation, University of Maryland, College Park, MD, USA, 2025.
- [18] H. Jamal Jumaah, W. Abbas Hasan, and S. Jamal Jumaah, "A Regional Investigation of Inverse Distance Weighting Particulate Matter Prediction within Kirkuk City, Iraq," *International Journal of Economic and Environmental Geology*, vol. 16, no. 1, pp. 5–13, Jan. 2025, <https://doi.org/10.46660/ijeege.v16i1.476>.
- [19] S. S. Ali and A. H. K. Albayati, "Statistical Modeling for Traffic Noise: The Case of Kirkuk City," *Engineering, Technology & Applied Science Research*, vol. 12, no. 5, pp. 9108–9112, Oct. 2022, <https://doi.org/10.48084/etasr.5173>.
- [20] M. F. M. Macêdo and A. L. D. Ramos, "Vehicle Atmospheric Pollution Evaluation Using AERMOD Model at Avenue in a Brazilian Capital City," *Air Quality, Atmosphere & Health*, vol. 13, no. 3, pp. 309–320, Mar. 2020, <https://doi.org/10.1007/s11869-020-00792-z>.
- [21] J. Miles, *WHO Global Air Quality Guidelines: Particulate Matter (PM<sub>2.5</sub> and PM<sub>10</sub>), Ozone, Nitrogen Dioxide, Sulfur Dioxide and Carbon Monoxide*, 1st ed. Geneva, Switzerland: World Health Organization, 2021.

- 
- [22] J. Salva, M. Vanek, M. Schwarz, M. Gajtanska, P. Tonhauzer, and A. Ďuricová, "An Assessment of the On-Road Mobile Sources Contribution to Particulate Matter Air Pollution by AERMOD Dispersion Model," *Sustainability*, vol. 13, no. 22, Nov. 2021, Art. no. 12748, <https://doi.org/10.3390/su132212748>.
- [23] K. O. Demirarslan, "Effects of Topographic Variables on Traffic-Related Pollutant Concentrations: Comparison of AERMOD and CAL3QHCR Models," *Frontiers in Environmental Science*, vol. 13, Jul. 2025, Art. no. 1577330, <https://doi.org/10.3389/fenvs.2025.1577330>.